



Complete One-Loop Corrections to $e^+e^- \rightarrow \tilde{\chi}_1^0 \tilde{\chi}_1^0 h^0$ for Different Scenarios

1T. A. Azim, 2S. M. Seif

Department of Physics, Faculty of Science, Cairo University, Giza, Egypt
taztabaz@sci.cu.edu.eg

Department of Physics, Faculty of Science, Cairo University, Giza, Egypt
sseif@sci.cu.edu.eg

ABSTRACT

In this work, the radiative corrections to the production of a light neutral Higgs boson (h^0) with a pair of lightest neutralinos ($\tilde{\chi}_1^0$) in e^+e^- collisions within MSSM are presented, including the on-shell renormalization scheme in the loop calculations. We have studied the QED corrections as well as the weak corrections, where the contribution from both corrections is significant and needs to be taken into account in the future linear colliders experiments. The result includes the numerical calculations for two different SUSY scenarios –Higgsino and Gaugino scenarios- for $e^+e^- \rightarrow \tilde{\chi}_1^0 \tilde{\chi}_1^0 h^0$.

Indexing terms/Keywords

Light neutral Higgs boson particle, Neutralinos, MSSM, QED, Weak interaction.

Academic Discipline And Sub-Disciplines

Elementary Particle Physics, High Energy Physics, Gauge Theories, Quantum Field Theory;

SUBJECT CLASSIFICATION

QC770-798, QC793-793.5

TYPE (METHOD/APPROACH)

Larg Hadron Collider (LHC), International Linear Collider (ILC), CMS and ATLAS Collaborations Publications.

INTRODUCTION 1

Linear electron-positron colliders are considered to be the best environment for precise studies of supersymmetric models, especially for the Supersymmetric Standard Model (MSSM). There are five Higgs mass states in MSSM: two CP-even, h^0 and H^0 , a CP-odd, A^0 and a pair of charged bosons, H^\pm . As clarified in [1, 2], all Higgs bosons in the MSSM, except the lightest CP-even one, are too heavy to play an important role in the current and the near future experiments. Therefore, the present study concentrates on the lightest Higgs boson h^0 only. On July 2012 [3–5], ATLAS and CMS teams at LHC have announced independently the discovery of a boson with the similar

properties of that of Higgs boson and confirmed likely, on March 2013, to be a Higgs boson of mass ~ 125 GeV.

This major breakthrough has a great impact on the searching for other supersymmetric particles and the mechanism of the supersymmetry (SUSY) breaking. The lightest MSSM CP-even Higgs particle mass is bounded from above and, depending on the SUSY parameters M_A and $\tan\beta$, is in the range of $m_h^{max} \approx 90 - 130$ GeV. The lower value comes from experimental constraints at LEP [6, 7], while the upper bound assumes a SUSY breaking scale $M_s \lesssim \mathcal{O}(1 \text{ TeV})$.

The mass of neutralinos is among the precision observables with lots of information on the SUSY-breaking structure, the relations between the particle masses and the SUSY parameters are important theoretical quantities for precision calculations. In MSSM [8], one has four neutralinos $\tilde{\chi}_1^0, \tilde{\chi}_2^0, \tilde{\chi}_3^0, \tilde{\chi}_4^0$, which are the fermion mass eigenstates of the supersymmetric partners of the photon, the Z^0 boson, and the neutral Higgs bosons h^0, H^0 . Their mass matrix depends on the parameters M_1, M_2, μ , and $\tan\beta$. If SUSY is realized in nature, neutralinos should be found in the present high energy experiments at Tevatron, LHC [9] and future e^+e^- colliders. Especially at a linear e^+e^- collider, it will be possible to perform measurements with high precision [10, 11].

To get high matching between the experimental predictions and theoretical calculations, it is unavoidable to include higher-order terms. In this paper, we use on-shell renormalization scheme in the loop calculations of the Higgs, neutralino sectors, and all SUSY particles of the CP-conserving MSSM. The calculation was performed using the FeynArts-3.6, FormCalc-7.1 and LoopTools-2.7 packages. At the one-loop level calculations, we have implemented all the renormalization constants, required to determine the various counterterms for the Higgs, neutralino and other sectors in the MSSM model file of FeynArts [12]. FormCalc was used to algebraically simplify the resulting amplitudes, which were converted to a FORTRAN program for integral evaluation using LoopTools.

The paper is arranged as follows: The analytical calculations of the electroweak radiative corrections to the $e^+e^- \rightarrow \tilde{\chi}_1^0 \tilde{\chi}_1^0 h^0$ process at one-loop level is given in section 2, involving the soft photonic corrections. The numerical results are presented in section 3. Finally, the conclusions are given in section 4.

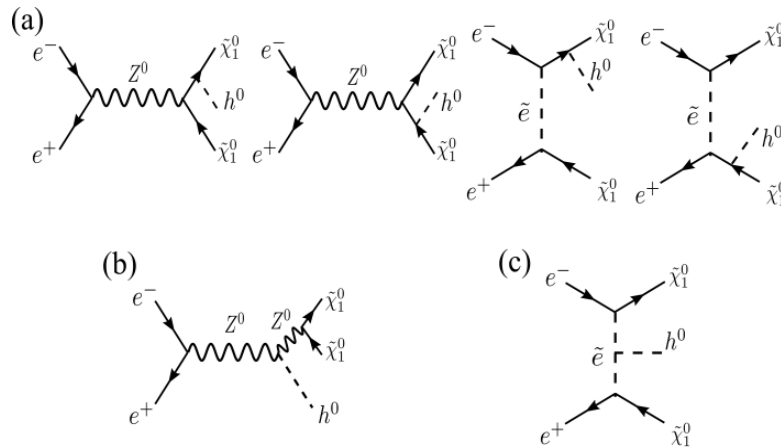


Fig 1: The lowest order (LO) Feynman diagrams for the $e^+e^- \rightarrow \tilde{\chi}_1^0 \tilde{\chi}_1^0 h^0$.

RADIATIVE CORRECTIONS 2

The associated production of MSSM neutral Higgs bosons with neutralinos is potentially substantial due to the large dependence of their coupling on the soft-SUSY breaking parameters, which are important theoretical quantities for precision calculations, and subsequently carry information on the SUSY theory [13].

The LO predictions for the cross sections suffer from large uncertainties because LO calculations has less precise results, so the higher order should be included. This process which is written as:

$$e^+(p_1) + e^-(p_2) \rightarrow \tilde{\chi}_1^0(p_3) + \tilde{\chi}_1^0(p_4) + h^0(p_5)$$

at the tree level are described by the Feynman diagrams of Fig.1. The momenta of the particles are given in brackets. The momenta obey the on-shell conditions $p_1^2 = p_2^2 = 0$, $p_3^2 = p_4^2 = m_{\tilde{\chi}_1^0}^2$, $p_5^2 = m_h^2$. The center-of-mass energy squared $s = (p_1 + p_2)^2$. The tree-level total cross section for this process can be written as:

$$\sigma^0(e^+e^- \rightarrow \tilde{\chi}_1^0 \tilde{\chi}_1^0 h^0) = \frac{(2\pi)^2}{4|\vec{p}_1|\sqrt{s}} \int \sum_{spin} |\mathcal{M}_0|^2 d\Phi_3 \quad (1)$$

where $d\Phi_3$ is the three-body phase space element

$$d\Phi_3 = \delta^4\left(p_1 + p_2 - \sum_{i=3}^5 p_i\right) \prod_{j=3}^5 \frac{d^3P_j}{(2\pi)^3 2E_j}.$$

Feynman diagrams in Fig. 1 represent the 6 most contributing topologies involved in this process:

- 3 with the s-channel Z^0 exchange,
- 3 with the t-channel left- and right-handed selectron $\tilde{e}_{L,R}$ exchange.

The diagrams where the h^0 boson is emitted from the electron and positron lines give negligible contributions.

For high precise results, radiative corrections should be included in the calculations which involve virtual one-loop correction and real photon emission such that:

$$\begin{aligned} \sigma &= \sigma^{virt} + \sigma^{real} \\ &= \int \sum_{spin} |\mathcal{M}_{virt}(e^+e^- \rightarrow \tilde{\chi}_1^0 \tilde{\chi}_1^0 h^0)|^2 d\Phi_3 + \int \sum_{spin} |\mathcal{M}_{real}(e^+e^- \rightarrow \tilde{\chi}_1^0 \tilde{\chi}_1^0 h^0 \gamma)|^2 d\Phi_4. \end{aligned} \quad (2)$$

One-loop Feynman diagrams can be classified as the following generic structure: The virtual vertex corrections Fig. 2, the box graph contributions to the propagators Fig. 3, and the self-energy contributions Fig. 4. The complete supersymmetric spectrum is used for the virtual particles inside loops. The evaluation of one-loop diagrams usually leads to two types of divergences:

- UV divergences, which are associated with singularities occurring at large loop momenta,
- IR divergences, which are generated, if one of the propagators in the loop vanishes.

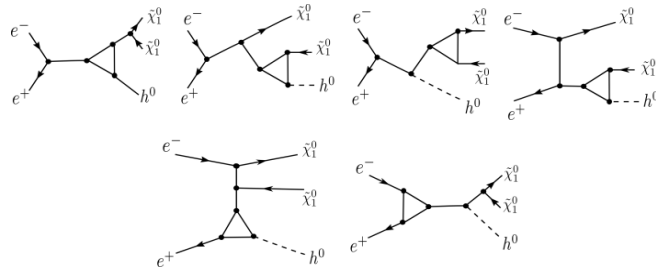


Fig 2: Vertex Corrections

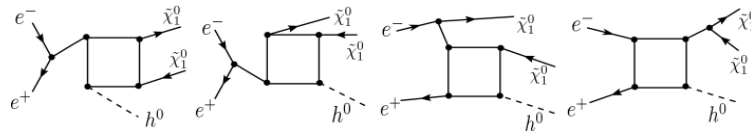


Fig 3: Box Corrections

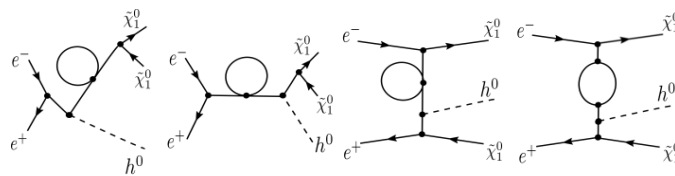


Fig 4: Self Corrections

To isolate the UV divergences, the regularization by dimensional reduction scheme (DR) is used to preserve SUSY. In this scheme only the momenta are treated as D -dimensional, while the fields and the Dirac algebra are kept 4-dimensional. To get rid of the UV divergences and absorb them, they should be renormalized by introducing a suitable set of counterterms for the renormalization of the coupling constants and the renormalization of the external wave functions. In this paper on-shell renormalization scheme is used in which all particle masses are defined as pole masses, such that the cross sections are directly related to the physical masses of the external particles and the other particles entering the loops [14], [15]. The complete cross section at the one-loop level can be written as follows:

$$\sigma^{1-loop} = \sigma^0 + \sigma^{virt} \quad (3)$$

The virtual electroweak radiative correction to the cross section is given by

$$\begin{aligned} \sigma^{virt} &= \sigma^0 \Delta_{virt} \\ &= \frac{(2\pi)^4}{2|\vec{p}_1|\sqrt{s}} \int d\Phi_3 \sum_{spin} Re(\mathcal{M}_0^\dagger \mathcal{M}_{virt}), \end{aligned} \quad (4)$$

where Δ_{virt} is the relative virtual correction and \mathcal{M}_{virt} is the renormalized amplitude involving all the one-loop electroweak Feynman diagrams and corresponding counterterms.

The contributions of virtual photon exchange in loops leads to soft IR divergences as well as the real photon emission [16], but their sum is IR finite. From previous discussion the corrected cross section can be expressed as following:

$$\sigma^{corr}(e^+e^- \rightarrow \tilde{\chi}_1^0 \tilde{\chi}_1^0 h^0) = \sigma^{ren}(e^+e^- \rightarrow \tilde{\chi}_1^0 \tilde{\chi}_1^0 h^0) + \sigma(e^+e^- \rightarrow \tilde{\chi}_1^0 \tilde{\chi}_1^0 h^0 \gamma)$$

Renormalization of Neutralino Sector 2.1

The tree level neutralino mass terms are given by:

$$\mathcal{L}_n = -\frac{1}{2}[\psi^{0I} Y \psi^0 + \bar{\psi}^{0I} Y^\dagger \bar{\psi}^0] + h.c.,$$

where

$$\psi^0 = (\tilde{B}^0, \tilde{W}^3, \tilde{h}_1^0, \tilde{h}_2^0)^T$$



Lagrangian involves the μ parameter, the soft-breaking gaugino-mass parameters M_1 and M_2 , and the Higgs vacua v_i , which are related to $\tan\beta = v_2/v_1$ and to the W mass $M_W = gv/2$ with $(v_1^2 + v_2^2)^{1/2}$ [15], [17].

After the electroweak symmetry is broken, the neutralino mass matrix in the bino–wino–higgsino basis can be written as:

$$Y = \begin{pmatrix} M_1 & 0 & -M_Z s_W \cos\beta & M_Z s_W \sin\beta \\ 0 & M_2 & M_Z c_W \cos\beta & -M_Z c_W \sin\beta \\ -M_Z s_W \cos\beta & M_Z c_W \cos\beta & 0 & -\mu \\ M_Z s_W \sin\beta & -M_Z c_W \sin\beta & -\mu & 0 \end{pmatrix},$$

which can be diagonalized with the help of a unitary 4×4 matrix N , yielding the neutralino mass eigenstates $\tilde{\chi}_i^0 (i = 1, \dots, 4)$.

Renormalization constants are introduced for the neutralino mass matrix Y and for the neutralino fields ψ^0 by the transformation:

$$Y \rightarrow Y + \delta Y, \\ \psi^0 \rightarrow \left(1 + \frac{1}{2} \delta Z_{\tilde{\chi}^0}\right) \psi^0. \quad (5)$$

where The matrix-valued renormalization constant $\delta Z_{\tilde{\chi}^0}$ is a general complex 4×4 matrix of one-loop order.

The physical (on-shell) masses are defined as poles of the real parts of the one-loop corrected propagators. The physical neutralino masses are then given by,

$$m_{\tilde{\chi}_i^0}^{os} = m_{\tilde{\chi}_i^0} + (N^* \delta Y N^{-1})_{ii} - \delta m_{\tilde{\chi}_i^0}, \quad (6)$$

where $m_{\tilde{\chi}_i^0}$ is the finite tree level mass, and $\delta m_{\tilde{\chi}_i^0}$ is the loop correction to the neutralino mass. The pole mass $m_{\tilde{\chi}_i^0}^{os}$ is considered as an input by specification of the parameters μ, M_1, M_2 , which are related to the input masses in the same way as in LO. In this way, the tree-level masses $m_{\tilde{\chi}_i^0}$ as well as the counterterm matrix δY , are fixed.

The matrix δY consists of the counterterms for the following parameters in the mass matrix Y : $M_1, M_2, \mu, \tan\beta$, the Z boson mass M_Z , W boson mass, which is involved in θ_W , and the electroweak mixing angle $s_W = \sin\theta_W, c_W = \cos\theta_W$, such that:

$$\delta Y = \begin{pmatrix} \delta M_1 & 0 & \delta Y_{13} & \delta Y_{14} \\ 0 & \delta M_2 & \delta Y_{23} & \delta Y_{24} \\ -\delta Y_{31} & \delta Y_{32} & 0 & -\delta\mu \\ \delta Y_{41} & -\delta Y_{42} & -\delta\mu & 0 \end{pmatrix}. \quad (7)$$

$\delta M_W^2, \delta M_Z^2$ and $\delta\theta_W$ are the same as in SM. We renormalize them according to the on-shell prescription of electroweak renormalization, where M_W and M_Z are physical (pole) masses, and $\cos\theta_W = M_W/M_Z$. This gives [18]:

$$\delta M_W^2 = \widetilde{\Re} \epsilon \Sigma_{WW}(M_W^2); \\ \delta M_Z^2 = \widetilde{\Re} \epsilon \Sigma_{ZZ}(M_Z^2); \\ \delta \cos\theta_W = \frac{M_W}{M_Z} \left(\frac{\delta M_W}{M_W} - \frac{\delta M_Z}{M_Z} \right). \quad (8)$$

Σ_{WW} and Σ_{ZZ} are the transverse components of the diagonal W and Z two-point functions in momentum space, respectively. Those three counterterms have, besides the contributions from the SM, new contributions from the MSSM involving loops of superparticles and additional Higgs bosons. $\delta\tan\beta$ is fixed in Higgs sector as following:

$$\delta\tan\beta = \frac{1}{2M_Z \cos^2\beta} \Im m(\Sigma_{AZ}(m_A^2)), \quad (9)$$

this implies that the two-point function connecting the CP-odd Higgs boson A to Z boson vanishes when A is on-shell.

$\delta M_1, \delta M_2$ and $\delta\mu$ are fixed in neutralinos sector. By using the three neutralino masses as inputs, the counterterms $\delta M_1, \delta M_2$ and $\delta\mu$ are all determined from Eq. (6).

Renormalization of Higgs Sector 2.2

As known the MSSM requires two Higgs doublets H_1 and H_2 with opposite hypercharge $Y_1 = -Y_2 = -1$. The quadratic part of the Higgs potential in the MSSM is given by:

$$V = m_1^2 H_1 \bar{H}_1 + m_2^2 H_2 \bar{H}_2 + m_{12}^2 (\epsilon_{ab} H_1^a H_2^b + h.c.) + \frac{1}{8} (g_1^2 + g_2^2) (H_1 \bar{H}_1 - H_2 \bar{H}_2)^2 - \frac{g_2^2}{2} |H_1 \bar{H}_2|^2, \quad (10)$$



where m_{12}^2 is defined to be negative and $\epsilon_{12} = -\epsilon_{21} = -1$, with soft breaking parameters m_1^2, m_2^2, m_{12}^2 and g_1, g_2 are, respectively, SU(2) and U(1) gauge couplings. Decomposing each Higgs doublet field $H_{1,2}$ in terms of its components [19], we get:

$$\begin{aligned} H_1 &= \begin{pmatrix} H_1^+ \\ H_1^0 \end{pmatrix} = \begin{pmatrix} (v_1 + \phi_1^0 - i\chi_1^0)/\sqrt{2} \\ -\phi_1^- \end{pmatrix}, \\ H_2 &= \begin{pmatrix} H_2^+ \\ H_2^0 \end{pmatrix} = \begin{pmatrix} \phi_2^+ \\ (v_2 + \phi_2^0 + i\chi_2^0)/\sqrt{2} \end{pmatrix}, \end{aligned} \quad (11)$$

The Higgs potential (5) is diagonalized by the rotations

$$\begin{aligned} \begin{pmatrix} H^0 \\ h^0 \end{pmatrix} &= \begin{pmatrix} \cos \alpha & \sin \alpha \\ -\sin \alpha & \cos \alpha \end{pmatrix} \begin{pmatrix} \phi_1^0 \\ \phi_2^0 \end{pmatrix} \\ \begin{pmatrix} G^0 \\ A^0 \end{pmatrix} &= \begin{pmatrix} \cos \beta & \sin \beta \\ -\sin \beta & \cos \beta \end{pmatrix} \begin{pmatrix} \chi_1^0 \\ \chi_2^0 \end{pmatrix} \\ \begin{pmatrix} G^+ \\ H^+ \end{pmatrix} &= \begin{pmatrix} \cos \beta & \sin \beta \\ -\sin \beta & \cos \beta \end{pmatrix} \begin{pmatrix} \phi_1^+ \\ \phi_2^+ \end{pmatrix}. \end{aligned} \quad (12)$$

G^0, G^\pm describe the unphysical Goldstone modes. The spectrum of physical states consists of: a light neutral CP-even state (h^0), a heavy neutral CP-even state (H^0), a neutral CP-odd state (A^0), and a pair of charged states (H^\pm). The masses of the gauge bosons and the electromagnetic charge are determined by

$$\begin{aligned} M_Z^2 &= \frac{1}{4}(g_1^2 + g_2^2)(v_1^2 + v_2^2), \\ M_W^2 &= \frac{1}{4}g_2^2(v_1^2 + v_2^2), \\ e^2 &= \frac{g_1^2 g_2^2}{g_1^2 + g_2^2}. \end{aligned} \quad (13)$$

Thus, the potential (10) contains two independent free parameters, which can conveniently be chosen as:

$$\tan \beta = \frac{v_2}{v_1}, \quad M_A^2 = -m_{12}^2(\tan \beta + \cot \beta), \quad (14)$$

where M_A is the mass of the A^0 boson.

Expressed in terms of Eq. (14), the masses of the other physical states are written as:

$$\begin{aligned} m_{H^0, h^0}^2 &= \frac{1}{2}[M_A^2 + M_Z^2 \pm \sqrt{(M_A^2 + M_Z^2)^2 - 4M_A^2 M_Z^2 \cos^2 2\beta}] \\ m_{H^\pm}^2 &= M_A^2 + M_W^2, \end{aligned} \quad (15)$$

and the mixing angle α in the (H^0, h^0)-system is derived from

$$\tan 2\alpha = \tan 2\beta \frac{M_A^2 + M_Z^2}{M_A^2 - M_Z^2}, \quad -\frac{\pi}{2} < \alpha \leq 0. \quad (16)$$

Hence, masses and couplings are determined by only a single parameter more than in the standard model.

The dependence on M_A is symmetric under $\tan \beta \leftrightarrow 1/\tan \beta$, and m_{h^0} is constrained by:

$$m_{h^0} < M_Z \cos 2\beta < M_Z. \quad (17)$$

This simple scenario, however, is changed when radiative corrections are taken into account.

The tree-level mass matrix m_0 of the neutral scalar system that represents bare mass system is diagonalized by Eqs. (12). Loop contributions to the quadratic part of the potential (neglecting the q^2 -dependence of the diagrams) modify the mass matrix as:

$$m_0 \rightarrow m_0 + \delta m = m. \quad (18)$$

Re-diagonalizing the one-loop matrix m yields the corrected mass eigenvalues m_{H^0, h^0} , replacing (10), and an effective mixing angle α_{eff} instead of (11). The renormalization constants [20] are defined as follows:

$$\begin{aligned} B_\mu &\rightarrow (Z_2^B)^{1/2} B_\mu, \\ W_\mu^a &\rightarrow (Z_2^W)^{1/2} W_\mu^a, \end{aligned}$$



$$\begin{aligned}
 H_i &\rightarrow Z_{H_i}^{1/2} H_i, \\
 \psi_j^L &\rightarrow (Z_L^j)^{1/2} \psi_j^L, \\
 \psi_{j\sigma}^R &\rightarrow (Z_R^{j\sigma})^{1/2} \psi_{j\sigma}^R, \\
 g_2 &\rightarrow Z_1^W (Z_2^W)^{-3/2} g_2, \\
 g_1 &\rightarrow Z_1^B (Z_2^B)^{-3/2} g_1, \\
 v_i &\rightarrow Z_{H_i}^{1/2} (v_i - \delta v_i), \\
 m_i^2 &\rightarrow Z_{H_i}^{-1} (m_i^2 + \delta m_i^2), \\
 m_{12}^2 &\rightarrow Z_{H_1}^{-1/2} Z_{H_2}^{-1/2} (m_{12}^2 + \delta m_{12}^2).
 \end{aligned} \tag{19}$$

The complete definitions and the explicit expressions of the renormalization constants of the other sectors: sfermion sector, MSSM parameters and fields including those of SM as the electric charge are treated as described in [21], to deliver all counterterms required for propagators and vertices appearing in the amplitudes.

Real Photon Emission 2.3

The soft IR divergences in the $\mathcal{M}_{\text{virtual}}$ in (4) originate from the contributions of virtual photon exchange in loops [22]. These soft (IR) divergencies can be cancelled by the real photon bremsstrahlung corrections in the soft photon limit. The real photonic emission process:

$$e^+(p_1) + e^-(p_2) \rightarrow \tilde{\chi}_1^0(p_3) + \tilde{\chi}_1^0(p_4) + h^0(p_5) + \gamma(k_\gamma),$$

where photon of momentum (k_γ) radiates from the electron/positron e^\pm , can have either soft or collinear nature. The collinear singularity is regularized by keeping electron (positron) mass.

The general phase-space-slicing method (PSS) is adopted to separate the soft photon emission singularity from the real photon emission processes. In the PSS approach the soft and collinear regions are excluded from phase space by appropriate phase-space cuts. By introducing an arbitrary small soft cutoff δ_s we separate the overall integration of the $2 \rightarrow 4$ phase space into singular and non-singular regions by the soft photon cut off, $\Delta E = \delta_s \sqrt{s}/2$, i.e. $E_\gamma \leq \Delta E$, or hard, i.e. $E_\gamma > \Delta E$. The real cross section of Eq. (2) can then be written as [23]:

$$\begin{aligned}
 \sigma^{\text{real}} &= \sigma^{\text{soft}}(\Delta E) + \sigma^{\text{hard}}(\Delta E) \\
 &= \sigma^0(\Delta_{\text{soft}} + \Delta_{\text{hard}})
 \end{aligned} \tag{20}$$

where σ^{soft} is obtained by integrating over the soft region of the photon phase space, and contains all the IR soft divergences of σ^{real} . To isolate the remaining collinear divergences from σ^{hard} , we further split the integration over the hard photon phase space according to whether the photon is (σ^{coll}) or is not ($\sigma^{\text{non-coll}}$) emitted within an angle θ with respect to the radiating particles such that $(1 - \cos \theta) < \delta_c$, for an arbitrary small collinear cutoff δ_c :

$$\sigma^{\text{hard}} = \sigma^{\text{coll}}(\theta) + \sigma^{\text{non-coll}}(\theta). \tag{21}$$

The hard non-collinear part of the real cross section, $\sigma^{\text{non-coll}}$, is finite and can be computed numerically, using standard Monte-Carlo techniques.

Due to the selectron exchange channels, one cannot separate off all Feynman diagrams with an additional photon attached to the tree-level diagrams to define pure “weak and QED corrections”, where we have $\sigma^{\text{weak}} = \sigma^{\text{soft}}$ and $\sigma^{\text{QED}} = \sigma^{\text{hard}}$. The energy of the radiated photon in the center of mass system frame is considered as a soft term, Δ_{soft} , with radiated photon energy $k_\gamma^0 < \Delta E$, and a hard term, Δ_{hard} , with $k_\gamma^0 > \Delta E$, where $k_\gamma^0 = \sqrt{|\vec{k}_\gamma|^2 + m_\gamma^2}$ and m_γ is the photon mass, used to regulate the IR divergences existing in the soft term.

In Eq. (20), ΔE depends largely on the weak and QED components. The main part of the QED corrections arises from the leading logarithms $L_e \equiv \log(s/m_e^2)$, resulting from photons in the beam direction. This leads to a large dependence on the experimental cuts and detector specifications. Therefore, we extract the ΔE and L_e terms, caused by collinear soft photon emission, from the weak corrections and add them to the QED corrections such that both corrections are now cutoff independent [24]. Now, Eq. (3) must be modified to include weak and QED corrections. The total renormalized one-loop cross section $\sigma^{1\text{-loop}}$ is expressed as:

$$\sigma^{1\text{-loop}} = \sigma^0 + \sigma^{\text{virt}} + \sigma^{\text{weak}} + \sigma^{\text{QED}}, \tag{22}$$

The integrated cross section at the one-loop level, can be written in the following way:

$$\sigma^{1\text{-loop}} = \sigma^0 + \sigma^0 \Delta, \tag{23}$$



where Δ , the relative correction, is given by

$$\Delta = (\sigma^{1-loop} - \sigma^0) / \sigma^0, \tag{24}$$

which can be decomposed into the following parts, indicating their origin,

$$\Delta = \Delta_{self} + \Delta_{vertex} + \Delta_{box} + \Delta_{QED} + \Delta_{weak} \tag{25}$$

NUMERICAL RESULTS 3

In present work, two different scenarios are studied. In the higgsino scenario, the neutralinos are higgsino-like as $\mu \ll M_1, M_2$ and the process is dominated by the s-channel Z_0 exchange. In the gaugino scenario the neutralinos are bino-like as $\mu \gg M_1, M_2$ the selectron exchange diagrams play the most important role. The renormalization scale is taken to be $Q = 2m_{\tilde{\chi}_1^0} + m_h$. The SM input parameters are set as the following: $\alpha(M_Z) = 1/127.922$, $M_e = 0.511$ MeV, $M_W = 80.399$ GeV, $M_Z = 91.187$ GeV, $M_t = 174.3$ GeV, $M_b = 4.7$ GeV.

The mass spectrum of the SUSY particles are set as shown in Tables 1 and 2 for Higgsino and Gaugino scenarios respectively using two programs Isajet, which is Monte Carlo program that simulates e^+e^- interaction, and SuSpect, which is Fortran code that calculates the supersymmetric and Higgs particle spectrum in MSSM. The free parameters that have been used in our calculations are specified as follows:

- All trilinear couplings are set to a common value A_f ($A_{tau} = A_b = A_t$), and all soft-SUSY-breaking parameters are assumed equal.
- The MSSM Higgs sector is parametrized by the CP-odd mass, m_A , and $\tan \beta$.
- The mixing between sfermion generations is neglected, $M_{SUSY} \equiv \tilde{M}_L \simeq \tilde{M}_R$.

Higgsino Scenario 3.1

The chosen SUSY parameters are set for Higgsino scenario as following: $M_2 = 400$ GeV, $\mu = -100$ GeV, $A_f = 400$ GeV, $\tan \beta = 10$, $m_A = 700$ GeV, $M_{SUSY} = 350$ GeV. The supersymmetric mass spectrum for Higgsino scenario using Isajet and SuSpect programs are set as shown in table 1.

Studying the dependency of the cross section on center of mass energy \sqrt{s} in Fig. 5 shows significant contributions from the Born approximation and the weak corrections, while the one-loop cross section has been suppressed due to QED corrections. Fig. 6 provides detailed study of the relation between the relative corrections of the cross section and \sqrt{s} . The highest value of the relative correction in the virtual part is due to the self-energy contribution.

The specific values of the maximum cross section and the related center of mass energy are shown in table 2. It shows that the weak correction has the highest value with $\sigma_{max} = 3.51 \times 10^{-6}$ pb at $\sqrt{s} = 700$ GeV, while the lowest value belongs to QED correction with $\sigma_{max} = 1.15 \times 10^{-6}$ pb at $\sqrt{s} = 650$ GeV.

Table 1: The mass spectrum of the SUSY particles for Higgsino scenario.

Particle	Mass/[GeV]	Particle	Mass/[GeV]
h^0	105.341	$\tilde{\chi}_1^0$	86.3240
H^0	700.275	$\tilde{\chi}_2^0$	111.646
A^0	700.000	$\tilde{\chi}_3^0$	200.218
H^\pm	704.600	$\tilde{\chi}_4^0$	416.025
\tilde{g}	1063.46	$\tilde{\nu}_e$	344.128
$\tilde{\chi}_1^\pm$	99.2230	$\tilde{\nu}_\mu$	344.128
$\tilde{\chi}_2^\pm$	416.032	$\tilde{\nu}_\tau$	342.105
\tilde{e}_L	352.582	\tilde{e}_R	353.214
$\tilde{\mu}_L$	352.519	$\tilde{\mu}_R$	353.277
$\tilde{\tau}_L$	349.346	$\tilde{\tau}_R$	356.424



\tilde{u}_L	345.881	\tilde{u}_R	348.268
\tilde{d}_L	350.860	\tilde{d}_R	354.925
\tilde{c}_L	345.667	\tilde{c}_R	348.485
\tilde{s}_L	350.853	\tilde{s}_R	354.932
\tilde{t}_L	281.995	\tilde{t}_R	469.650
\tilde{b}_L	343.316	\tilde{b}_R	362.288

Table 2: The maximum cross section in Higgsino scenario.

	$(\sigma)_{max} / \text{Pb}$	\sqrt{s} / GeV
Born	2.82×10^{-6}	700
1-loop	3.28×10^{-6}	700
QED	1.15×10^{-6}	650
Weak	3.51×10^{-6}	700

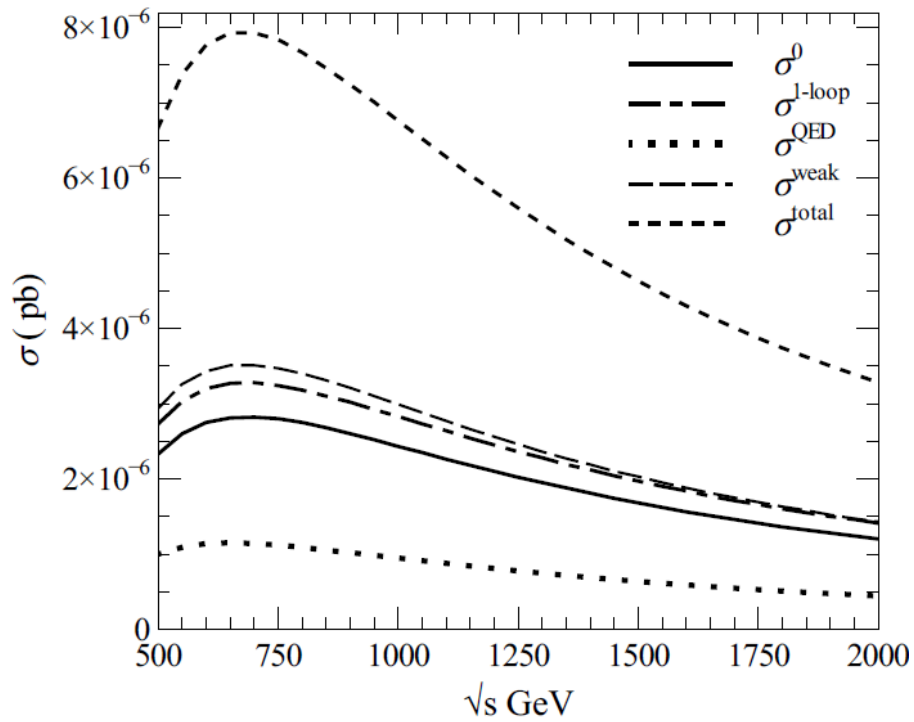


Fig 5: Total cross section as a function of \sqrt{s} in the Higgsino scenario.

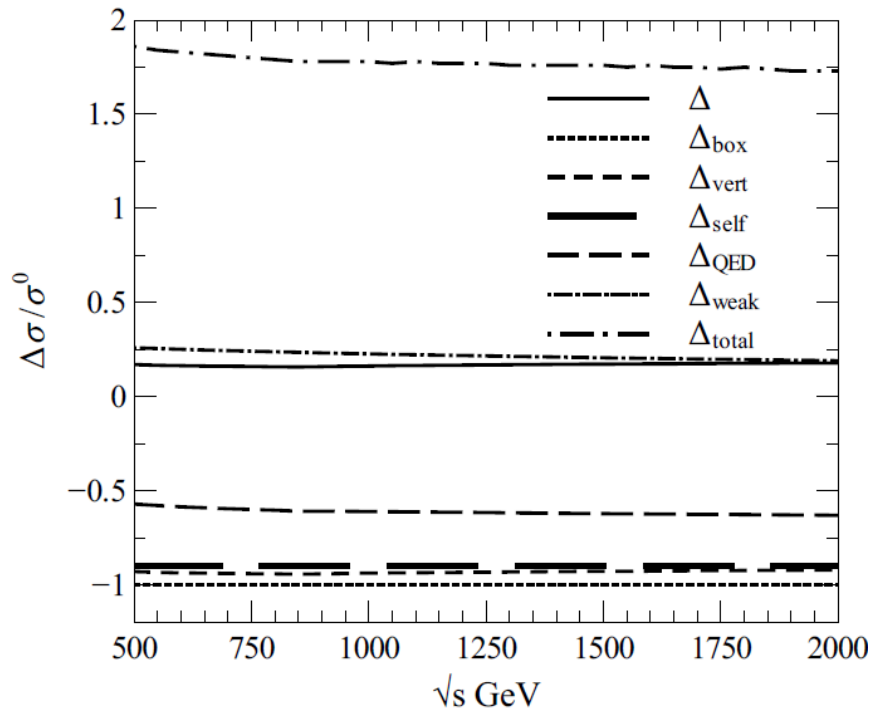


Fig 6: Relative corrections as a function of \sqrt{s} in the Higgsino scenario.

Gaugino Scenario 3.2

The chosen SUSY parameters are set for Gaugino scenario as following: $M_2 = 197.6$ GeV, $\mu = 353.1$ GeV, $A_f = -100$ GeV, $\tan \beta = 10.2$, $m_A = 393.6$ GeV, $M_{SUSY} = 500$ GeV.

The supersymmetric mass spectrum for Gaugino scenario using the same programs, Isajet and SuSpect, are set as shown in table 3.

In this scenario, studying the dependency of the cross section on \sqrt{s} , Fig. 7, reveals that the Born approximation beside the QED and weak corrections enhanced the value of one-loop correction, where the weak correction contributes with the highest value while the QED correction has the lowest. In Fig. 8, the relative corrections for the three types of one-loop correction have approximately the same values in the range of $\sqrt{s} > 1000$ GeV, while beyond this value the virtual vertex correction has the highest value.

Table 4 shows that the one-loop correction has the highest value with $\sigma_{max} = 1.21 \times 10^{-7}$ pb at $\sqrt{s} = 1000$ GeV, while QED correction the lowest value with $\sigma_{max} = 5.65 \times 10^{-8}$ pb at $\sqrt{s} = 850$ GeV.

Table 3: The mass spectrum of the SUSY particles for Gaugino scenario.

Particle	Mass/[GeV]	Particle	Mass/[GeV]
h^0	110.985	$\tilde{\chi}_1^0$	91.5340
H^0	393.987	$\tilde{\chi}_2^0$	181.009
A^0	393.600	$\tilde{\chi}_3^0$	359.502
H^\pm	401.727	$\tilde{\chi}_4^0$	378.874
\tilde{g}	525.351	$\tilde{\nu}_e$	495.905
$\tilde{\chi}_1^\pm$	180.516	$\tilde{\nu}_\mu$	495.905
$\tilde{\chi}_2^\pm$	379.562	$\tilde{\nu}_\tau$	495.905



\tilde{e}_L	501.812	\tilde{e}_R	502.257
$\tilde{\mu}_L$	501.586	$\tilde{\mu}_R$	502.483
$\tilde{\tau}_L$	495.440	$\tilde{\tau}_R$	508.551
\tilde{u}_L	497.123	\tilde{u}_R	498.787
\tilde{d}_L	500.591	\tilde{d}_R	503.475
\tilde{c}_L	497.107	\tilde{c}_R	498.807
\tilde{s}_L	500.557	\tilde{s}_R	503.508
\tilde{t}_L	504.356	\tilde{t}_R	548.374
\tilde{b}_L	484.474	\tilde{b}_R	519.044

Table 4: The maximum cross section in Gaugino scenario.

	$(\sigma)_{max} / \text{Pb}$	\sqrt{s} / GeV
Born	8.59×10^{-8}	1050
1-loop	1.21×10^{-7}	1000
QED	5.65×10^{-8}	850
Weak	1.05×10^{-7}	1000

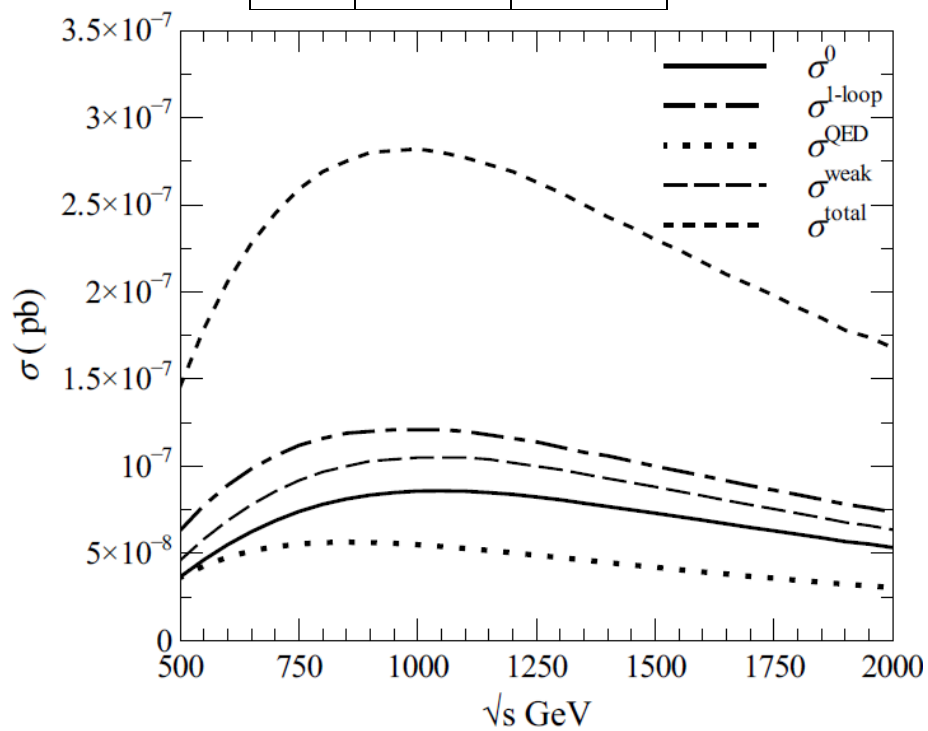


Fig 7: Total cross section as a function of \sqrt{s} in the Gaugino scenario.

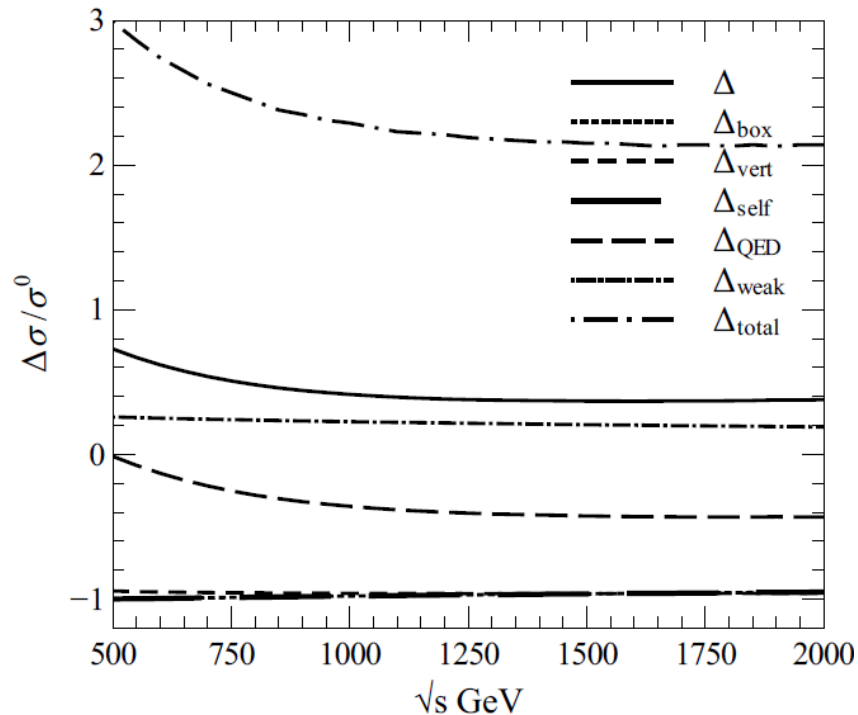


Fig 8: Relative corrections as a function of \sqrt{s} in the Gaugino scenario.

CONCLUSIONS 4

In this paper we calculate the full electroweak radiative corrections at one-loop level to the lightest neutralino pair production with light neutral Higgs boson at electron-positron LC in the frame of MSSM. The calculations were performed in an analytical method using the FeynArts-3.6 and FormCalc-7.1 computer packages, where we modified the MSSM model file implemented in FeynArts-3.6 by adding the renormalization constants and counterterms of all MSSM particles. We have calculated the weak and QED corrections, which contribute significantly to the total cross section.

The full one-loop corrections are in the range of 12-20% for Higgsino scenario, and of 40-70% for Gaugino scenario, thus they have to be taken into account in future linear collider experiments. The maximum cross sections are presented in Tables 3 and 4 for both scenarios. In general, by comparing the cross section values of the two scenarios, it is found that Higgsino scenario has larger values for all types of correction than that of the Gaugino scenario. The complete one-loop corrections for the Gaugino scenario are in the range of 20-30% for the same reaction according to ref. [25], showing the effect of the chosen parameters on the calculations.

ACKNOWLEDGMENTS

We would like to express our sincere gratitude to our advisor Pro. Dr. M. Khaled Hegab, and our thanks to Pro. Dr. Samiha Abou Stiet for revising the paper linguistically. We have to express our appreciation to Dr. Ibrahim A. Abdul-Magead for sharing his fruitful thoughts.

REFERENCES

1. Nakamura, K. et al. 2010. Particle Data Group (2010) Review of particle physics.
2. Egijyan, G. K., Jurcisin, and M., Kazakov, D. I. 1999. Infrared Quasi Fixed Points and Mass Predictions in the MSSM.
3. Beringer, J. et al. 2012. Review of Particle Physics.
4. LEP collaborations 2003. Search for the Standard Model Higgs Boson at LEP.
5. Cho, A. 2012. Higgs Boson Makes Its Debut After Decades-Long Search.
6. The ATLAS Collaboration 2012. Observation of a new particle in the search for the Standard Model Higgs boson with the ATLAS detector at the LHC.
7. The ATLAS Collaboration 2012. Combined search for the Standard Model Higgs boson in pp collisions at $\sqrt{s} = 7$ TeV with the ATLAS detector.
8. Nilles, H. P. 1984. Supersymmetry, supergravity and particle physics;



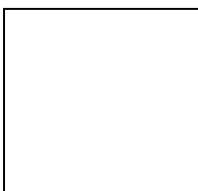
- Haber, H. E. and Kane, G. L. 1985. The search for supersymmetry: Probing physics beyond the standard model.
9. The ATLAS Collaboration 2014. Search for direct production of charginos, neutralinos and sleptons in final states with two leptons and missing transverse momentum in pp collisions at $\sqrt{s} = 8$ TeV with the ATLAS detector.
 10. Heuer, R. -D. et al. 2001. TESLA Technical Design Report Part III: Physics at an e^+e^- Linear Collider.
 11. Adolphsen, C. et al. 2000, International study group progress report on linear collider development.
 12. Hahn, T. and Schappacher, C. 2002. The implementation of the Minimal Supersymmetric Standard Model in FeynArts and FormCalc.
 13. Beskidt, C., de Boer, W., and Kazakov, D.I. 2014. The impact of a 126 GeV Higgs on the neutralino mass.
 14. Choi, S.Y. et al. 2000, Reconstructing the Chargino System at e^+e^- Linear Colliders;
Moortgat-Pick, G. et al. 2001, Analysis of the Neutralino System in Supersymmetric Theories.
 15. Fritzsche, T. and Hollik, W. 2002. Complete one-loop corrections to the mass spectrum of charginos and neutralinos in the MSSM.
 16. Hollik, W. and Rzehak, H. 2003. The sfermion mass spectrum of the MSSM at the one-loop level.
 17. Fritzsche, T. and Hollik, W. 2004. One-loop calculations for SUSY processes;
Fritzsche, T. 2004. Complete one-loop calculations in the chargino/neutralino sector of the MSSM. The International Conference on Linear Colliders.
 18. Marciano, W. and Sirlin, A. 1980. Radiative corrections to neutrino-induced neutral-current phenomena in the $SU(2)_L \times U(1)$ theory.
 19. Dabelstein, A. 1995. The one-loop renormalization of the MSSM Higgs sector and its application to the neutral scalar Higgs masses.
 20. Farzinnia, A., He, H., and Ren, J. 2013. Natural Electroweak Symmetry Breaking from Scale Invariant Higgs Mechanism.
 21. Denner, A. 1993. Techniques for the calculation of electroweak radiative corrections at the one-loop level and results for W-physics at LEP200.
 22. 't Hooft, G. and Veltman, M. 1979. Scalar one-loop integrals;
Jing-Jing, L. et al. 2007. Full one-loop electroweak corrections to $h^0(H^0, A^0)H^\pm W^\mp$ associated productions at e^+e^- linear colliders.
 23. Giele, W. T. and Glover, E. W. N. 1992. Higher-order corrections to jet cross sections in e^+e^- annihilation;
Giele, W. T., Glover, E. W., and Kosower, D. A. 1993. Higher Order Corrections to Jet Cross Sections in Hadron Colliders.
 24. Denner, A. and Dittmaier, S. 1993. Electroweak radiative corrections to $e^-\gamma \rightarrow W^- \nu_e$;
Böhm, M. and Dittmaier, S. 1993. The Hard bremsstrahlung process $e^-\gamma \rightarrow W^- \nu_e$.
 25. Seif, S. M., Azim, T. A., and Abdul-Magead, I. A. 2014. One-Loop Corrections for Production of a Light neutral MSSM Higgs Boson with a Pair of Neutralinos at the e^+e^- Linear Collider.

Author,s Biography



Prof. Tarek Abd El-Azim Abd El-Maksoud Ibrahim.

Professor at Department of Physics, Faculty of Science, Cairo University,
Giza, Egypt.
E-mail: taztabaz@sci.cu.edu.eg



Dr. Shymaa Mohammed Mohammed Seif.

Teacher at Department of Physics, Faculty of Science, Cairo University,
Giza, Egypt.
E-mail: sseif@sci.cu.edu.eg